

# Dynamic Contrast Enhanced and Diffusion Weighted MRI from Primary Tumors and Metastatic Cervical Lymph Nodes in Squamous Cell Carcinomas of the Head and Neck

S. Chawla<sup>1</sup>, S. Kim<sup>1,2</sup>, L. Dougherty<sup>1</sup>, S. Wang<sup>1</sup>, L. A. Loevner<sup>1</sup>, H. Quon<sup>3</sup>, and H. Poptani<sup>1</sup>

<sup>1</sup>Radiology, University of Pennsylvania, Philadelphia, PA, United States, <sup>2</sup>Radiology, New York University, New York, NY, United States,

<sup>3</sup>Radiation Oncology, University of Pennsylvania, Philadelphia, PA, United States

**Introduction:** Dynamic contrast-enhanced MRI (DCE-MRI) derived volume transfer constant ( $K^{trans}$ ) and diffusion weighted imaging (DWI) has been used in characterization<sup>1,2</sup>, monitoring treatment response<sup>3-5</sup> and in prediction of survival<sup>6</sup> in squamous cell carcinomas of head and neck (HNSCC) patients. However, majority of these studies have reported  $K^{trans}$  and ADC values from metastatic cervical lymph nodes<sup>2-4</sup>. In comparison to the metastatic node,  $K^{trans}$  and apparent diffusion coefficient (ADC) measurements from primary tumor are challenging, as these tumors are generally located in areas prone to artifacts induced by continuous physiologic motion. The current DCE-MRI study was performed using a radial imaging technique along with dynamic K-space weighted image reconstruction contrast (KWIC)<sup>7</sup> to reduce motion sensitivity and assess the primary tumor mass. In addition, motion correction algorithms<sup>8</sup> were performed to further reduce motion artifacts in the DCE-MRI and DWI data. Correlation analysis of  $K^{trans}$  and ADC from the primary tumor and metastatic node was then performed to assess the utility of these methods in the primary tumor site.

**Methods:** Twenty-eight patients with HNSCC underwent anatomical imaging, DCE-MRI and DWI. DCE-MRI was performed using a fast 3D spoiled gradient-echo sequence, which was modified to acquire eight angle-interleaved sub-aperture images from the full-echo radial data. The imaging parameters were: 256 readout points/view, 256 views (32 views/subaperture, 8 subapertures), fat saturation was applied once every 8 excitations. Spatial saturation was applied once every 32 excitations to minimize the flow effect while minimizing the scan time. This data acquisition scheme resulted in a temporal resolution of 2.5 s for each sub-aperture image with full spatial resolution of  $256 \times 256$  by using KWIC algorithm.<sup>3,9</sup> Gd-DTPA was injected at a dose of 0.1 mmol/kg body weight at 1 ml/s followed by saline flush, during which scanning was continued for another 9 minutes. DWI was acquired using a pulsed gradient spin-echo/echo planar imaging sequence with three b values: 0, 500, and 1,000  $s/mm^2$ . Pharmacokinetic model analysis of DCE-MRI data was performed to generate pixel wise  $K^{trans}$  maps using the generalized kinetic model<sup>10</sup>. Similarly, pixel by pixel ADC maps were also computed. All anatomical images,  $K^{trans}$  and ADC maps were co-registered using a two-step non-rigid image registration technique to minimize motion artifacts. First 3D registration with affine transformation was performed to minimize global misalignment. Subsequently, a fine 2D registration scheme were applied.<sup>8,9</sup> Furthermore, view dependent phase correction methods were applied to reduce both rotational and translational motions.<sup>8</sup> Median pretreatment  $K^{trans}$  and ADC values were computed from regions of interest on the primary tumors and largest nodal masses. Spearman's correlation analyses were performed for  $K^{trans}$  and ADC values between primary tumors and nodal masses. **Results:** Co-registered anatomical images,  $K^{trans}$  and ADC maps from a representative HNSCC patient are shown in Figure 1. We observed a significantly high correlation ( $r=0.684$ ,  $p<0.001$ ) for  $K^{trans}$  between primary tumors and nodal masses. Moderate but significant correlation ( $r=0.407$ ,  $p=0.031$ ) was also observed between ADC of primary tumors and lymph nodes (Fig. 2).

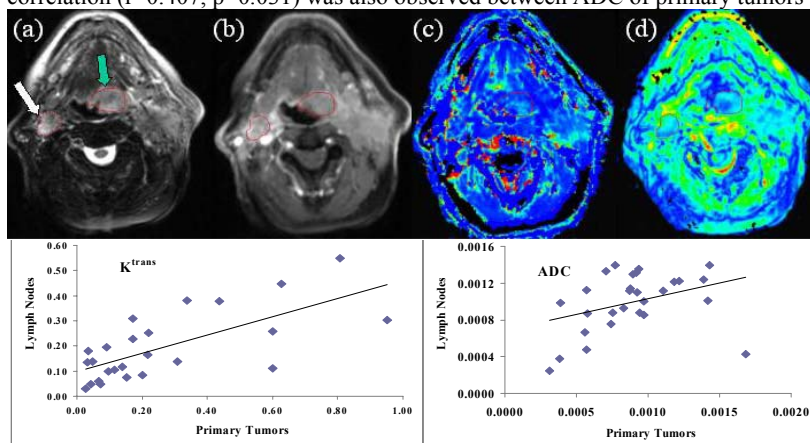


Figure1: Axial T2-weighted image (a) demonstrating heterogeneous hyperintense primary tumor (green arrow) and metastatic lymph node (white arrow) at level IIa of neck. These masses exhibit heterogeneous enhancement on post-contrast T1-weighted image (b). Corresponding DCE-MRI derived  $K^{trans}$  map (c) and ADC map (d) from these lesions. Figure 2: Scatter plots demonstrating strong positive correlation for  $K^{trans}$  and ADC between primary tumors and lymph nodes

**Discussion and Conclusion:** In spite of greater vulnerability of DCE-MRI being corrupted due to motion from primary tumors, we observed good quality of  $K^{trans}$  maps in 89.28% of the cases (only 3 of the 28 cases had to be dropped because of severe motion). We used radial pulse sequence to minimize motion artifacts as well as to achieve a high temporal resolution of 2.5s. Moreover, motion correction methods and non-rigid registration were also used to eliminate the misalignment among the anatomical images and parametric maps. We believe that combination of these two approaches substantially improves the estimation of  $K^{trans}$  from both primary tumors and nodal masses. Significant correlations of  $K^{trans}$  and ADC values between primary tumors and nodal masses suggest that both lesions have similar biological and physiological characteristics. As several head and neck cancer patients only have a lesion at the base of tongue (N=0 staging), the ability to achieve high quality  $K^{trans}$  and ADC maps from these regions may aid in evaluating diagnostic and prognostic role of DCE-MRI and DWI in primary tumors.

**References:** [1]Hoskin PJ, Br J Radiol 1999;72:1093-98; [2]Sumi M et al. Am J Roentgenol, 2006;186:749-57; [3]Kim S et al. Am J Neuroradiol, 2010;31:262-8; [4]Kim S et al. Clin Cancer Res. 2009;15:986-94; [5]Cao Y et al. Int J Radiat Oncol Biol Phys 2008;72:1287-90; [6]Vandecaveye V et al. Eur Radiol, 2010 ;20:1703 14; [7]Song HK et al. Magn Reson Med 2004;52:815-24. [8]Kim S et al. Magn Reson Imaging, 2008;26:367-78 [9]Kim S et al. J Magn Reson Imaging, 2007;26:1607-17; [10]Tofts PS et al. J Magn Reson Imaging, 1999;10:223-32.